The synthesis of sulfated titanium oxide nanotubes

Chiu-Hsun Lin [a,*], Shu-Hua Chien [b], Jiunn-Hsing Chao [c], Chyi-Yang Sheu [a], Yu-Cheng Cheng [a], Ya-Jean Huang [a], and Chih-Hsiang Tsai [a]

[a] Department of Chemistry, National Changhua University of Education, Changhua 500, Taiwan
[b] Institute of Chemistry, Academia Sinica, Nankang Taipei 11529, Taiwan
[c] Nuclear Science and Technology Development Center, National Tsing Hua University, Hsinchu 300, Taiwan

Received 8 November 2001; accepted 13 February 2002

TiO_2 nanotubes can be prepared in gram quantities by treating anatase TiO_2 powder with concentrated NaOH solution. These TiO_2 nanotubes acquired strong acidity after being impregnated with sulfuric acid solution and calcined at 300 °C. The anatase TiO_2 powder used to prepare the nanotube did not catalyze the esterification between cyclohexanol and acetic acid, while sulfated TiO_2 nanotubes were very reactive toward the esterification reaction.

KEY WORDS: sulfated; titanium oxide; anatase; nanotube.

1. Introduction

The synthesis of a material with a well-defined nanoscale cavity is currently under intensive investigation. The recent discovery of carbon nanotubes [1] has promoted numerous research efforts in this field because of the diverse potential uses of the nanotubes in microscope probe tips, microelectronic devices, catalysis, and as a hydrogen storage device [2]. Recently, micro- and nanotubes of inorganic oxides including TiO_2 [3–5], MnO_2 [4], Co_3O_4 [4], MoO_3 [6], V_2O_5 [4,6,7], Al_2O_3 [6], ZrO_2 [8], and SiO_2 [6,9] have been prepared. TiO_2 nanostructured material, in particular, is of great interest in catalysis [4,10,11], photovoltaic cells [12] and semiconductor devices [13]. This paper focuses on the catalytic aspect of the material.

It has been reported [11] that TiO_2 with a smaller particle size had a better catalytic performance. Strong-acid sites were created on a nanometer-sized anatase and their activation energy for 1-butene isomerization decreased with a decrease in TiO_2 crystallite size. The acidity of TiO_2 was enhanced upon being promoted with WO_3 or MoO_3, and so was its photocatalytic activity for the degradation of harmful 1,4-dichlorobenzene in aqueous solution [14]. Sulfate-promoted TiO_2 possessed very strong acidity and was able to catalyze the isomerization of butane at room temperature [15]. From the catalysis viewpoint, it will be most rewarding if we can promote TiO_2 nanotubes with sulfate groups so that these nanotubes become acidic. The acidity and the tubular structures of the nanotube may enable these sulfate-promoted TiO_2 nanotubes to function like a zeolite catalyst. In this paper, we want to report a method for preparing an acidic sulfated TiO_2 nanotube.

* To whom correspondence should be addressed.
E-mail: chlin@cc.ncue.edu.tw

2. Experimental

2.1. Preparation of the sulfated titanium oxide nanotubes

3.0 g of anatase TiO_2 powder were mixed with 200 ml of 10 M NaOH solution in a perfluoroalkoxy container and stirred for 20–30 h at 110 °C. The resulting paste was filtered, neutralized with 0.1 M HCl solution and washed in deionized water a few times to remove the NaCl formed. To prepare sulfated nanotubes, the filter cake after the final deionized water washing was further washed with 0.01 M H_2SO_4 solution, filtered and dried at 110 °C for 24 h. The dried powder was exposed to 0.5 M H_2SO_4 using a ratio of 1.0 g of powder to 15 ml of the sulfuric acid solution [15]. The resulting H_2SO_4/TiO_2 powder was dried at 110 °C and then calcined at elevated temperatures to obtain the final sulfated TiO_2 nanotubes.

2.2. Characterization of titanium oxide nanotubes

SEM and TEM images were obtained with a Hitachi S-2460N scanning electron microscope and a JEOL JEM-2000FXII transmission electron microscope, respectively. Oxford Exl10/T energy-dispersive X-ray (EDX) was used to analyze the elemental constituents of the nanotube. Surface composition of the nanotube was obtained using a Qmicron X-ray photoelectron spectroscopy (XPS) system equipped with an Mg K_α 1253.6 eV X-ray source. XRD experiments were performed on a Scintag DMS 2000 diffractometer equipped

1011-372X/02/0600-0153/0

with Cu K_α radiation. The Na^+ and sulfur concentrations in the prepared TiO_2 nanotube were estimated by neutron activation analysis and ICP-AES, respectively. BET surface areas were obtained with an ASAP 2010 surface area and porosimetry analyzer. Esterification reaction was carried out using 0.5 g of the catalysts, 59.2 mmol of acetic acid and 27.5 mmol of cyclohexanol in toluene under reflux condition.

3. Results and discussion

TiO_2 nanotubes were synthesized by the template method [3,4] and the chemical process method [5]. In the former method, an organic surfactant molecule or an Al_2O_3 membrane with a straight pore must be used as a template during the synthesis of the nanotube. These organic or inorganic templates had to be removed at the end of the preparation by calcining, solvent extraction, or dissolving in a basic solution. In the latter, milligrams of needle-shaped TiO_2 nanotubes (8 nm in diameter and 100 nm in length) were produced by contacting fine SiO_2–TiO_2 particles with an alkali solution in a sealed stainless steel digestion bomb without using any template. Because of the very small size of this discrete needle-shaped TiO_2 nanotube, it is difficult for it to be used as a catalyst. We were able to prepare a fibrous TiO_2 nanotube in gram quantity by utilizing an anatase TiO_2 powder as the starting material. Since such material could be prepared in gram quantity per synthesis run and the length of the prepared TiO_2 nanotubes was in the micrometer range, utilizing this material as a catalyst in the laboratory was quite straightforward.

Figures 1(a) and 1(b) show SEM images of the TiO_2 nanotubes prepared by our method after neutralizing with diluted HCl solution and washing with deionized water. As clearly seen in figure 1(a), numerous fiber-like nanotubes grew from a micron-size TiO_2 particle. These nanotubes had an outer diameter between 10 and 100 nm and a length between 2 and 18 μm. A close-up of these nanotubes is shown in figure 1(b). A TEM image of a TiO_2 nanotube near its tube opening is presented in figure 1(c). The hollow nature of the nanotube is clearly visible in the TEM image. This TiO_2 nanotube had an average wall thickness of 12 nm and an inner free diameter of 16 nm. The total pore volume of the nanotube was estimated to be 0.98 ml g^{-1} by absorption of water. X-ray diffraction indicated that this TiO_2 material was composed mainly of the anatase phase and the rutile was only the minor component, similar to the starting TiO_2 powder. Neutron activation analysis indicated that there were about 3600 ppm of Na^+ left in the prepared TiO_2 nanotube. Therefore, the nanotube was rinsed with a diluted H_2SO_4 solution to further reduce the sodium content before impregnating with the sulfate.

It needs to be pointed out that since these fibrous TiO_2 nanotubes are numerous and lie close to each other, they tend to stick to each other, forming a raft-like material after filtering and drying at 110 °C, as shown in figure 1(d). Nonetheless, these steps did not deform the morphology of the individual nanotube. Calcination up to 300 °C did not seem to cause severe sintering. For example, the starting TiO_2 powder had a BET surface area of 10 $m^2 g^{-1}$, but that of the TiO_2 nanotubes in figure 1(d) was 258 $m^2 g^{-1}$ and that of the one calcined at 300 °C was 238 $m^2 g^{-1}$. SEM and TEM images (figures 1(e) and 1(f)) showed that both nanotube morphology and the hollow pore structure remained intact after calcination at 300 °C.

The formation of the long TiO_2 nanotubes was possibly through a "dissolution and growth" mechanism. When the anatase powder contacted with 10 M

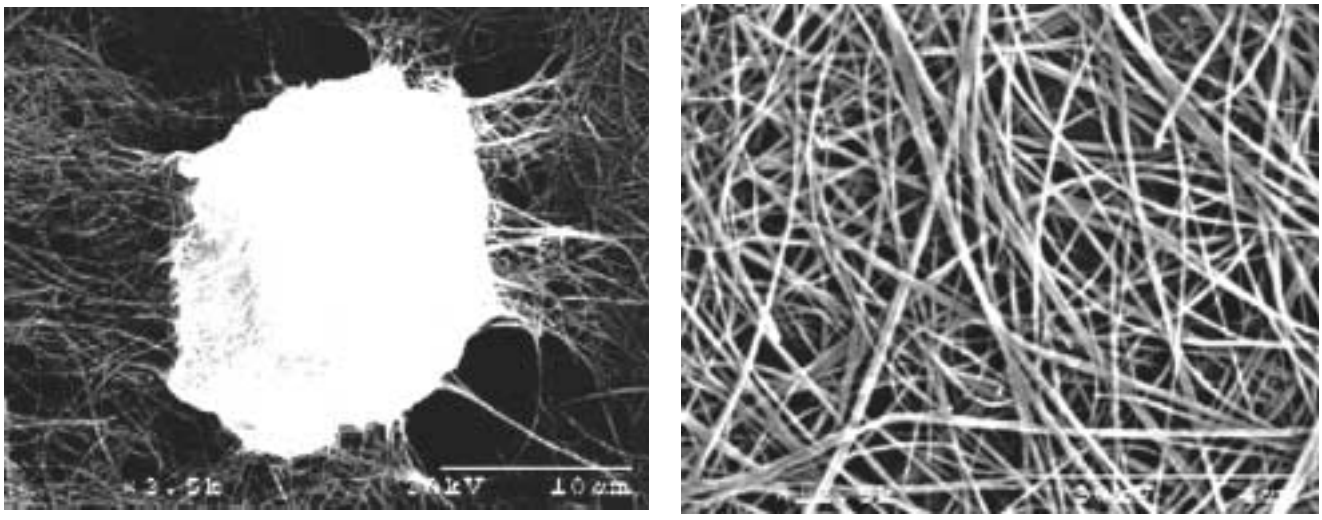

(a) (b)

Figure 1. (a) SEM image of TiO_2 nanotubes after washing and neutralization, (b) SEM image of a close-up of the nanotubes.

(c)

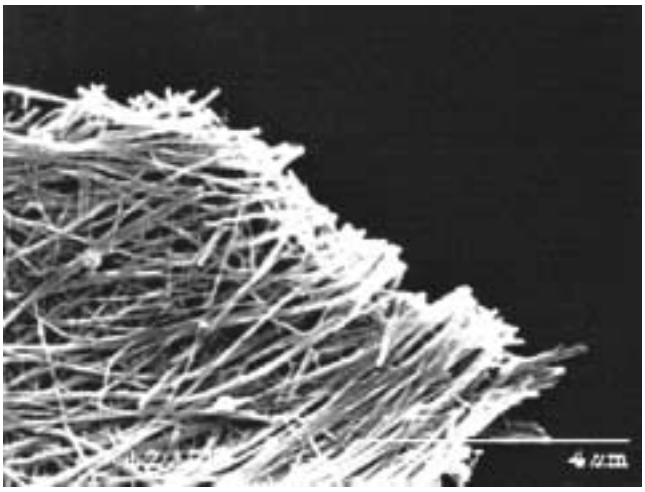

(d)

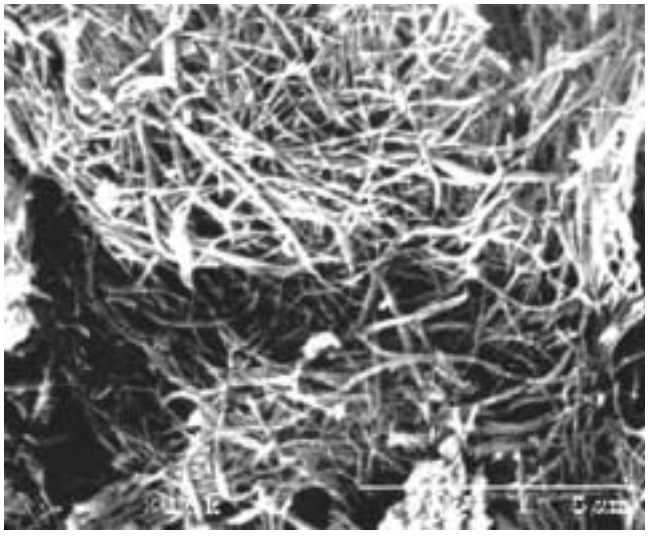

(e)

(f)

Figure 1 (continued). (c) TEM image of a single nanotube near its tube opening, (d) SEM image of TiO_2 nanotubes after filtration and drying at 110 °C, (e) SEM image of TiO_2 nanotubes calcined at 300 °C, (f) TEM image of TiO_2 nanotubes calcined at 300 °C.

NaOH, the TiO_2 particles were severely corroded and dissolved in the strong alkali solution. As the dissolution process proceeded, the Ti–O–Ti bonds in TiO_2 were broken and some Ti species accumulated in the NaOH solution, which ultimately led to the redeposition of these Ti species and the growth of short TiO_2 nanotubes on the TiO_2 particle surface as shown in figure 2(a) (bright spots). Figure 2(a) was obtained by stirring 3 mg of anatase powder in 10 M NaOH for 5–6 h. The formation of the short nanotube was more clearly visible if the TiO_2 and NaOH mixture was not stirred and reacted steadily for 20 h (figure 2(b)). The TiO_2 particles in figure 2(b) were not as extensively corroded as in figure 2(a), and the short nanotubes on the particle surface had a diameter between 30 and 40 nm and were about 100–200 nm in length. The reason for the occurrence of the short nanotubes was not clear, but anatase TiO_2 is tetragol with a unit cell parameter of $a = b = 3.784$ Å, and

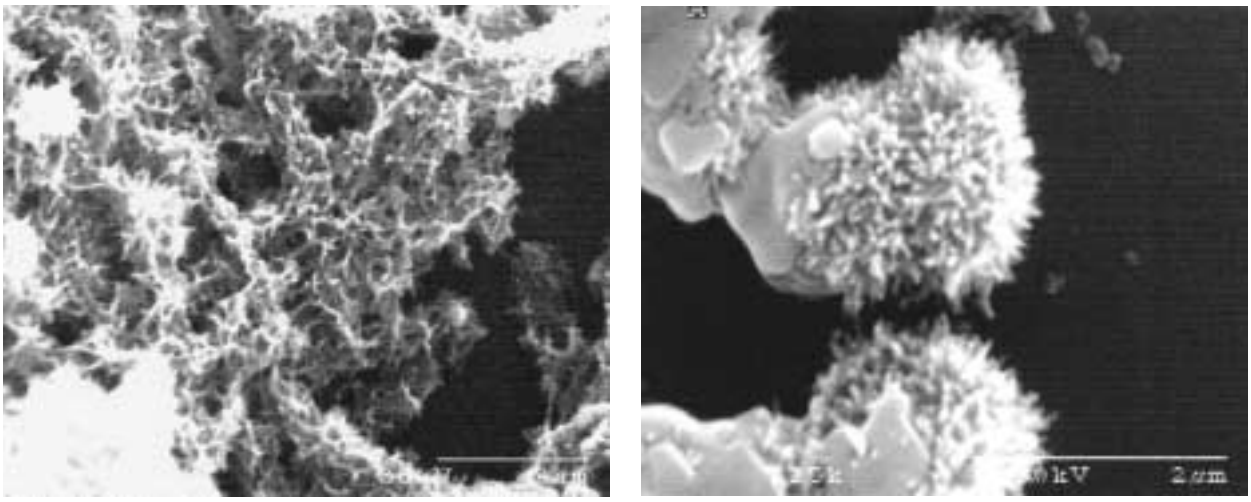

(a) (b)

Figure 2. (a) SEM image of 3 mg TiO_2 anatase powder treated in 12 ml of stirring 10 M NaOH solution for 6 h at 110 °C, (b) SEM image of the reaction mixture of (a) at 110 °C for 20 h without stirring.

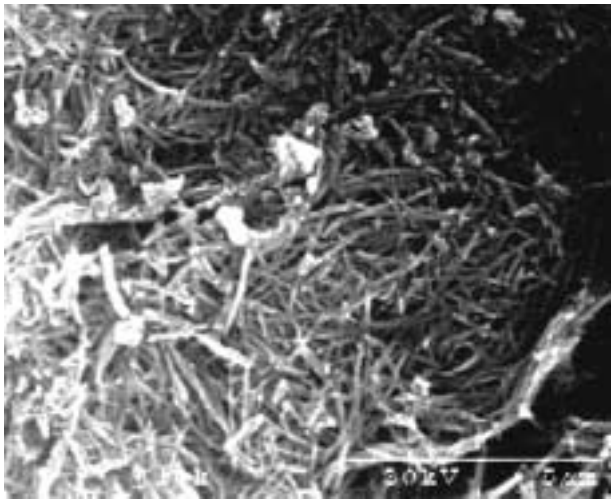

(a)

(c)

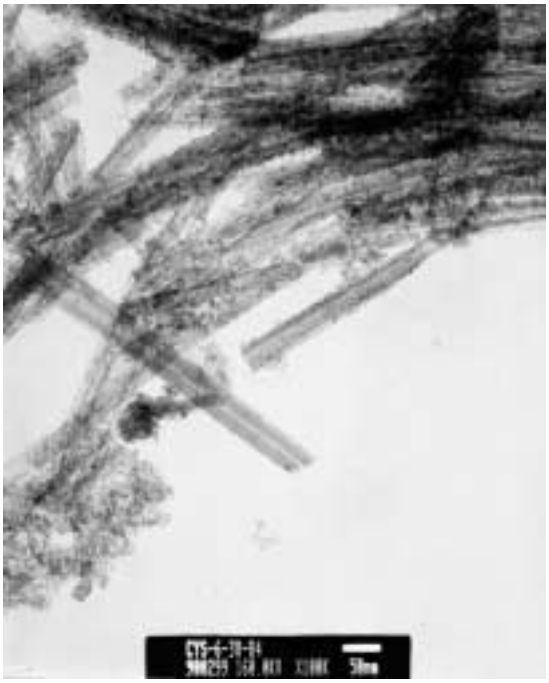

(b)

Figure 3. (a) SEM image of sulfated TiO_2 nanotubes calcined at 300 °C, (b) TEM image of sulfated TiO_2 nanotubes calcined at 300 °C, (c) SEM image of a used sulfated TiO_2 nanotube catalyst after 10 h reaction.

$c = 9.515$ Å. Since the c axis is much larger than the other two directions, anatase TiO_2 may prefer to grow in certain directions in favor of formation of the short nanotube during the dissolution–growth process. When reaction was under stirring and a larger amount of TiO_2 was dissolved to produce a high concentration of the Ti species in the alkali solution, the short nanotube could serve as the template to grow the observed micrometer-sized TiO_2 long nanotubes. The formation of our nanotube seems to be different from what Kasuga observed: that the nanotube was formed during the washing process [5].

To prepare sulfated titania catalyst, we had impregnated our TiO_2 nanotubes with H_2SO_4 aqueous solution and calcined at elevated temperatures. SEM and TEM images of the sulfated TiO_2 nanotubes calcined at 300 °C are presented in figures 3(a) and 3(b). The hollow portion of the sulfated TiO_2 nanotube is still clearly visible in figure 3(b). The nanotube located at the lower left corner in figure 3(b) has an average wall thickness of 15 nm and an inner free diameter of 8 nm. XRD indicated that such sulfated nanotubes consisted of mostly the anatase phase. The sulfur signal was detected in the tube section of the impregnated material by EDX (figure 4). In addition to the Ti, O, and S signal, the EDX spectrum also indicated the presence of some Si impurity. ICP-AES analysis on a digested sample showed that the material contained 3.2 wt% of sulfur. XPS was used to characterize the surface composition of the sulfated TiO_2 nanotube. A binding energy of $S(2p_{3/2})$ was observed at 168.1 eV with $S(2p_{1/2})$ at 169.9 eV as a shoulder. These values are typical of S^{+6} such as those in Na_2SO_4 and $Al_2(SO_4)_3$ [16]. The binding energies for $Ti(2p_{3/2})$ and $Ti(2p_{1/2})$ were at 458.9 eV and 464.0 eV, respectively, with a difference of 5.10 eV. These values are consistent with those reported for Ti in TiO_2 [16]. There are two peaks in the O(1s) core-level binding energy region: the one at 529.7 eV belongs to the oxidic oxygen in TiO_2 and the other, appearing as a shoulder peak of the former at 531.1 eV, was attributed to the sulfate oxygen. The XPS spectra of the sulfated TiO_2 nanotubes calcined at 300, 400 and 500 °C are shown in figure 5. These XPS results led to the conclusion that the surface species on the sulfated TiO_2 nanotube was a sulfate group.

The acid strength of a sulfated titanium oxide calcined at 300 °C was estimated to be −12.70 on a Hammett color indicator scale [17]. The acidic nature of SO_4^{-2}/TiO_2 powder was demonstrated by its being capable of increasing the rate of some acid-catalyzed reactions [15,17,18]. We utilized the esterification of cyclohexanol with acetic acid to demonstrate the acidic nature of the sulfated TiO_2 nanotube. The esterification reaction data are depicted in figure 6. The anatase TiO_2 powder was not reactive toward the esterification reaction as its ester yield was similar to that of a blank reaction (without the presence of a catalyst). On the other hand, the ester

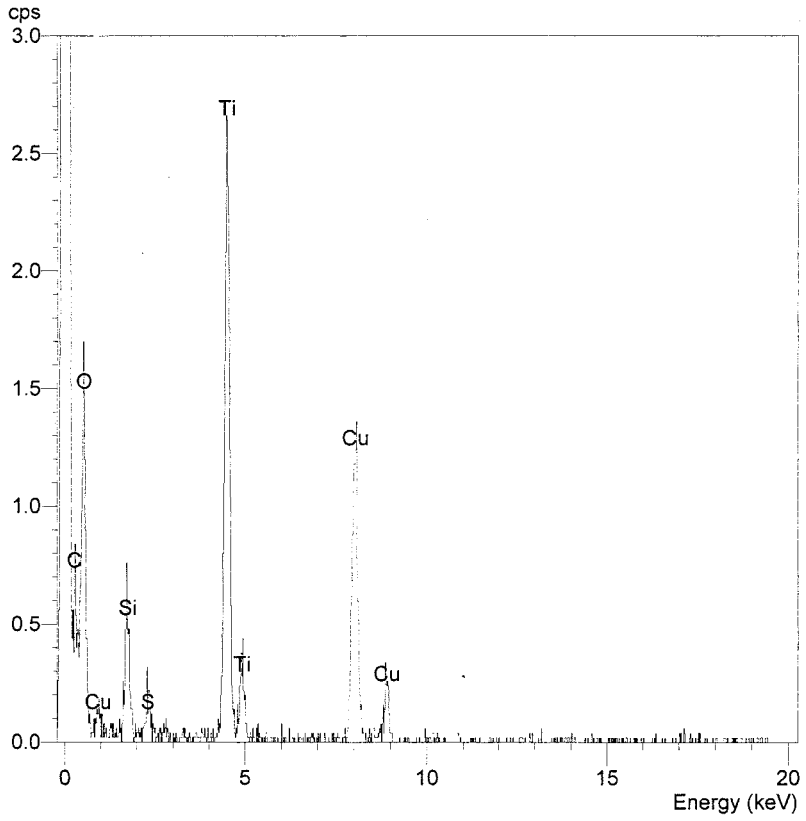

Figure 4. EDX spectrum of sulfated TiO_2 nanotubes calcined at 300 °C.

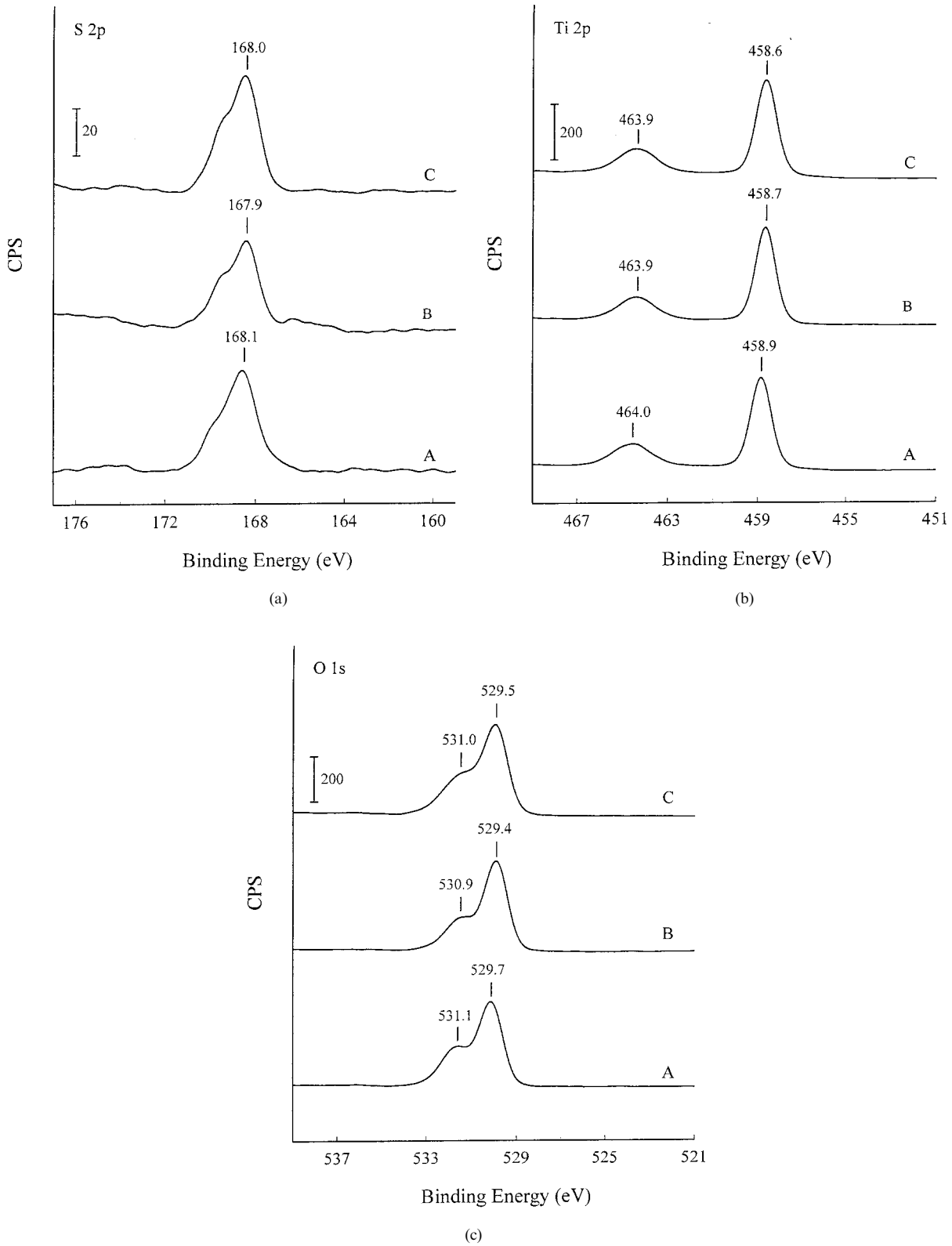

Figure 5. The XPS spectra of the sulfated TiO_2 nanotubes calcined at (a) 300 °C, (b) 400 °C and (c) 500 °C.

yield of the sulfated TiO_2 nanotube rose from 13% at the first hour of reaction to 55% at the end of the tenth hour. The acidic nature of the sulfate-modified TiO_2 nanotube is clearly demonstrated here. Other preliminary reaction results indicate that the larger surface area and pore size of the sulfated TiO_2 nanotube might be beneficial for the reaction involving organic molecules of larger size. It is interesting to point out that the nanotube morphology of the sulfated nanotube remained intact after 10 h of reaction (figure 3(c)).

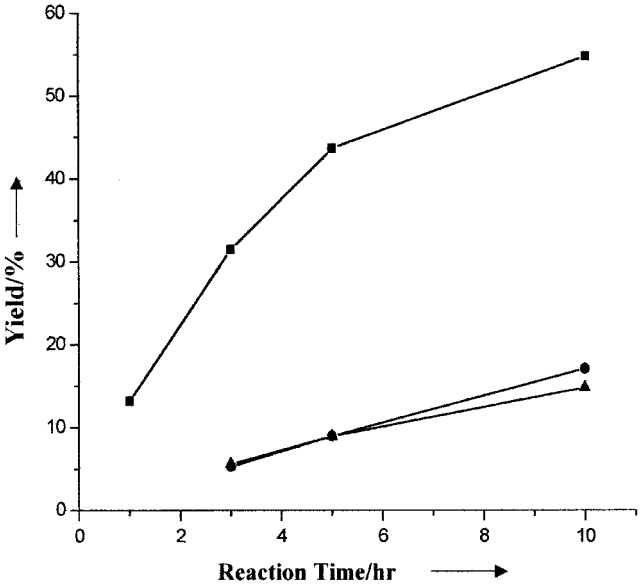

Figure 6. Esterification of the acetic acid with cyclohexanol catalyzed by different catalysts: ■, sulfated TiO_2 nanotubes calcined at 300 °C; ●, anatase TiO_2 powder; ▲, blank reaction.

In summary, fibrous TiO_2 nanotubes and sulfated TiO_2 nanotubes could be prepared in gram quantity without using a template molecule. The acidity of the latter was verified by its being able to catalyze the esterification reaction. The possible roles of the acidity and tubular pore structure of this TiO_2 nanotube in catalyzed reactions are presently under investigation.

Acknowledgments

C.-H.L. is grateful for technical assistance from Professor J.-C. Wu of the Physics Department at NCUE, and he is also grateful for a grant to support this research from the National Science Council of Taiwan (NSC-89-2113-M-018-015).

References

[1] S. Iijima, Nature 354 (1991) 56.
[2] C.N.R. Rao, B.C. Satishkumar, A. Govindaraj and M. Nath, Chem. Phys. Chem. 2 (2001) 78.
[3] S. Kobayashi, K. Hanabusa, N. Hamasaki, M. Kimura and H. Shirai, Chem. Mater. 12 (2000) 1523.
[4] B.B. Lakshmi, C.J. Patrissi and C.R. Martin, Chem. Mater. 9 (1997) 2544.
[5] T. Kasuga, M. Hiramatsu, A. Hoson, T. Sekino and K. Niihara, Langmuir 14 (1998) 3160.
[6] B.C. Satishkumar, A. Govindaraj, E.M. Vogl and L. Basumallick, C.N.R. Rao, J. Mater. Res. 12 (1997) 604.
[7] M.E. Spahr, P. Bitterli, R. Nesper, M. Muller, F. Krumeich and H.U. Nissen, Angew. Chem. 110 (1998) 1339.
[8] C.N.R. Rao, B.C. Satishkumar and A. Govindaraj, Chem. Commun. (1997) 1581.
[9] H. Nakamura and Y. Matsui, J. Am. Chem. Soc. 117 (1995) 2651.
[10] M. Adachi, Y. Murata, M. Harada and S. Yoshikawa, Chem. Lett. (2000) 942.
[11] H. Nakabayashi, N. Kakuta and A. Ueno, Bull. Chem. Soc. Jpn. 64 (1991) 2428.
[12] A. Hagfeldt and M. Gratzel, Chem. Rev. 95 (1995) 49.
[13] K. Vinodgopal, S. Hotchandani and P.V. Kamat, J. Phys. Chem. 97 (1993) 9040.
[14] J. Papp, S. Soled, K. Dwight and A. Wold, Chem. Mater. 6 (1994) 496.
[15] M. Hino and K. Arata, Chem. Commun. (1979) 1148.
[16] J.F. Moulder, W.F. Stickle, P.E. Sobol and K.D. Bomben, *Handbook of X-ray Photoelectron Spectroscopy* (Perkin-Elmer Corp., USA, 1992), p. 236.
[17] C. Guo, S. Yao, J. CaO and Z. Qian, Appl. Catal. A: General 107 (1994) 229.
[18] R. Li, J. Chen, W. Zhang, H. Yang, Z. Zhao and Q. Wei, React. Kinet. Catal. Lett. 48 (1992) 483.